BJRS

BRAZILIAN JOURNAL
OF
RADIATION SCIENCES
10-02A (2022) 01-17

Ethylene-vinyl acetate detector exposed to gamma radiation and evaluated *via* principal component regression

Oliveira[a,b,*] L.N., Nascimento[a] E.O., Antonio[b] P.L., and Caldas[b] L.V.E

[a] *Instituto Federal de Educação, Ciência e Tecnologia de Goiás – IFG, 74055-110, Goiânia - GO, Brazil*

[b] *Instituto de Pesquisas Energéticas e Nucleares – IPEN/CNEN, 05508-000, São Paulo - SP, Brazil*

lucas@ifg.edu.br

ABSTRACT

Ethylene-vinyl acetate (EVA) is the flexible plastic material commonly used in industries. The EVA samples, in green, white and black colors were irradiated with absorbed doses of 0.01 kGy up to 10.0 kGy using a ^{60}Co Gamma Cell-220 system, and the Fourier Transform Infrared (FTIR) spectrophotometry technique was used for evaluating the samples. This work aimed to investigate EVA samples in measurements with gamma radiation, analyzing the linearity through the Principal Component Regression (PCR) method and its sensitivity. For sensitivity and linearity, the green samples showed the best results, followed by white and black EVA samples. The PCR method inflated gradually the number of principal components, then reducing the residuals between the measured and calculated values, consequently obtaining maximum linearity of 1.000 for all of the EVA samples. In conclusion, the FTIR was adequate for the acquisition of absorbance spectra; the linearity via PCR and sensitivity showed good results indicating that the EVA detectors can be useful in radiation measurements.

Keywords: **Ethylene-vinyl acetate (EVA), Radiation dosimetry, PCR analyses, FTIR technique.**

ISSN: 2319-0612
DOI: https://10.15392/bjrs.v10i2A.1760
Submitted:2021-11-05
Accepted: 2022-03-14

1. INTRODUCTION

Applications of ethylene-vinyl acetate (EVA) has been commonly evaluated in radiation physics research such as in electron beam irradiations [1–5], UV measurements [6], and microwave irradiation [7]. The gamma radiation is well known and has several applications in radiation dosimetry [7–10]. In this way, after choosing the dosimetric system and its range for the irradiations, it is necessary to evaluate it; the evaluation of EVA and other dosimeters can be done by the Fourier Transform Infrared (FTIR) spectrophotometry technique [11,12]. EVA is a polymeric material which presents characteristics such as high flexibility [13], and good shielding properties [14]; it is widely used as rubber in various engineering structures; its chemical and physical properties are of interest in several areas of science [15,16]. A characteristic of the EVA is that the values of the ratio of mass energy absorption coefficients change with energy only slightly [17]; this fact is important in dosimetry especially in calibrations at different energies, when the dosimeter used could be water equivalent.

Typically, dosimeters employed in radiation measurements must have characteristics as to be easily applied in medical physics; in this regard, a linear relation as a function of absorbed dose is one of the most valuable features [18–22]. Linearity provides important information such as in which regions the dosimeter can be used [23,24]; the sensitivity indicates ranges within the spectra where the absorbance showed high dispersion to the absorbed doses [25–27]. In this way, mathematical methods can be useful to find optimal regions with high linearity [28–31], so that the dosimeter can be investigated in linear regions that previously could not be analyzed. One of these methods is the Principal Component Regression (PCR) that provides a multidimensional relation for the input data to the output, by minimizing the effects of redundant information through multicollinearity reduction [32]. After centralizing the data and consequently reducing the dimensionality, the PCR method applies linear regression; this PCR result is important for cases of dosimeters that are used in radiation dosimetry. Information on the application of PCR in dosimetry can be found in the literature [33].

The objective of this work was to investigate gamma radiation in green, white, and black EVA dosimeter samples for their sensitivity and linearity response, using the PCR method, and evaluated with the FTIR spectrophotometry technique.

2. MATERIALS AND METHODS

The EVA samples had dimensions of 0.5 x 0.5 x 0.1 cm^3, in colors green, white and black. These samples were irradiated in triplicates, with absorbed doses of 0.01 kGy, 0.05 kGy, 0.10 kGy, 0.25 kGy, 0.50 kGy, 1.0 kGy, 5.0 kGy and 10.0 kGy using a ^{60}Co Gamma Cell-220 system (dose rate of 1.089 kGy/h), at the Radiation Technology Center of IPEN; afterwards, the absorbance spectrum of each sample was acquired on a Fourier Transform Infrared (FTIR) Spectrometer (Frontier/Perkin Elmer), from 400 cm^{-1} to 4000 cm^{-1}, with 1 cm^{-1} spectral resolution, and with an attached Attenuated Total Reflection (ATR) equipament.

The linearity was evaluated using the Pearson correlation coefficient (R^2). The sensitivity was set as the linear coefficient from a simple linear regression that was fitted using the Ordinary Least Squares Method (OLSM) between the absorbed doses and absorbance values for each wavenumber in the spectra for all colors of EVA samples, respectively. Seeking to compare the EVA color samples, the sensitivity was normalized between -1 and +1.

The PCR method combines all spectra from absorbance measurements into a single matrix, called here as X_{nm}, where n is the absorbed dose that varied discreetly from n = 1 up to 8, matching the absorbed doses of 0.01 kGy, 0.05 kGy, 0.10 kGy, 0.25 kGy, 0.50 kGy, 1.0 kGy, 5.0 kGy and 10.0 kGy, m is the spectral resolution index, from m = 1 up to 3600, that is equivalent to the range from 400 cm^{-1} to 4000 cm^{-1}; more details about the algorithm and its applications can be found in the literature [34]. In this work, X matrix was standardized by the mean-centering normalization and adjusted by the standard deviation. The PCR was made with the possibility of adjusting eigenvector quantities, in this case, called *k* (1 up to 8) which is the number of absorbed doses by the EVA samples. The multivariate analysis was done in Matlab 2020a. The Mean Squared Error (MSE) was used to calculate the prediction accuracy of the PCR method; this is a well-established error metric [35]. The MSE is a function of the number of principal components (k); so, for each evaluated k, one corresponding value to MSE was obtained. The residuals were calculated for the PCR subtracting the measured and predicted values as a function of absorbed dose, associated with the number of principal components (*k*), that in this work was modified in connection with the number of absorbed doses in measurements (k = 1 up to k = 8).

3. RESULTS AND DISCUSSION

Figure 1 shows FTIR spectra, absorbance *versus* wavenumber, for EVA a) green, b) white and c) black samples, irradiated with absorbed doses from 0.01 kGy to 10.0 kGy (^{60}Co source). The average absorbance response from the triplicate measurement for each absorbed dose is shown, and the uncertainty obtained through the relative standard deviation was lower than 1%. After performing an inspection in Figure 1 it was possible to find regions with peak absorbance, in which the absorbed dose was more significant. These EVA samples did not change their color with gamma radiation exposure in the analyzed region. From these results the vibrational mode for C-H asymmetric and symmetrical stretching at 2964 and 2862 cm^{-1} respectively can be inferred too. Other results and applications of the vibrational mode can be found in the literature [36].

a)

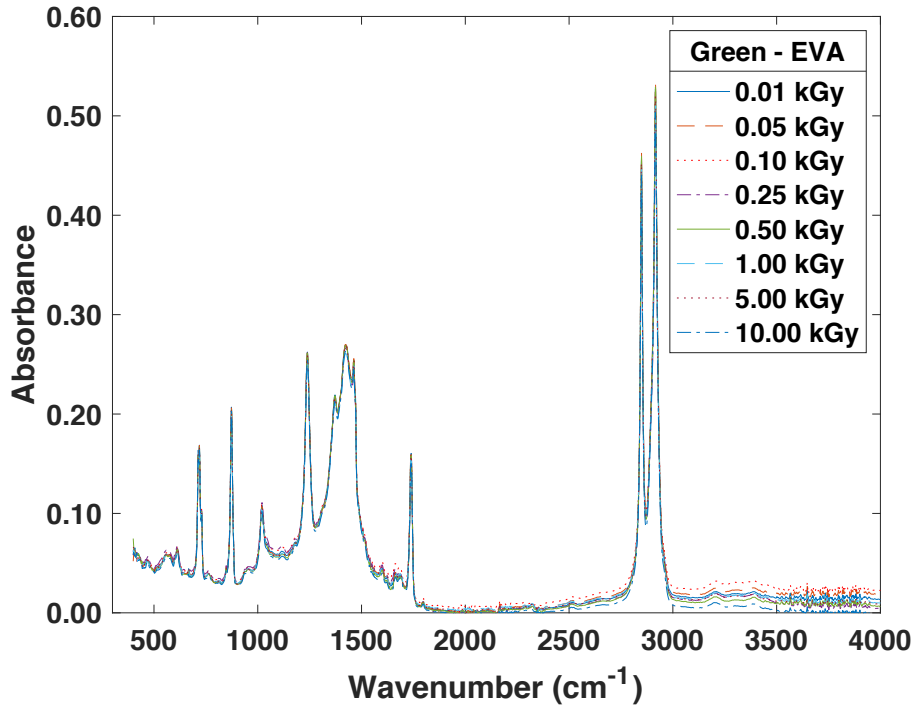

b)

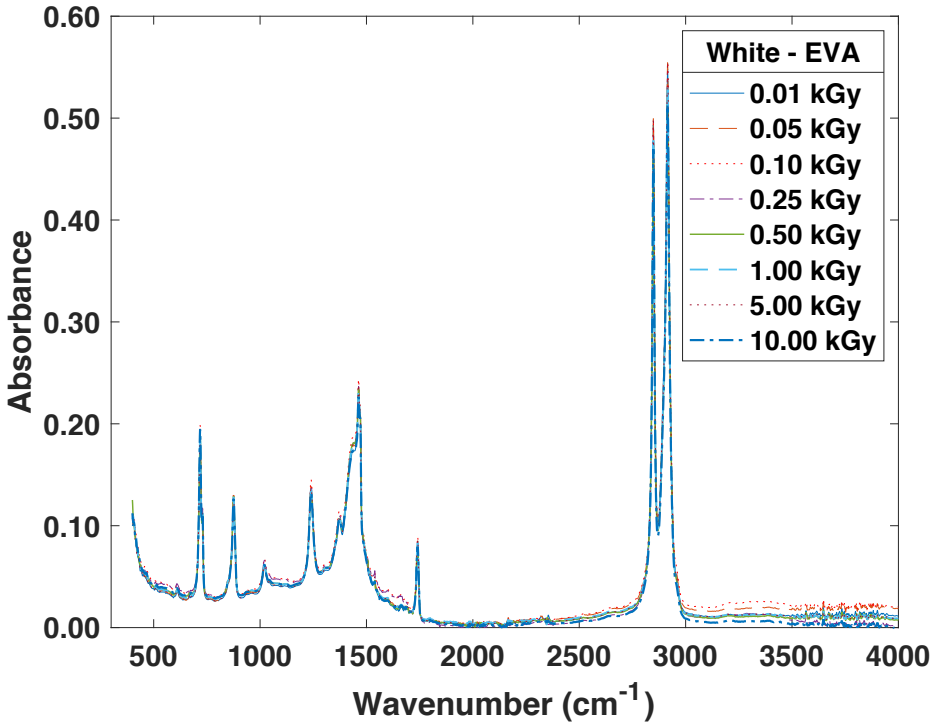

c)

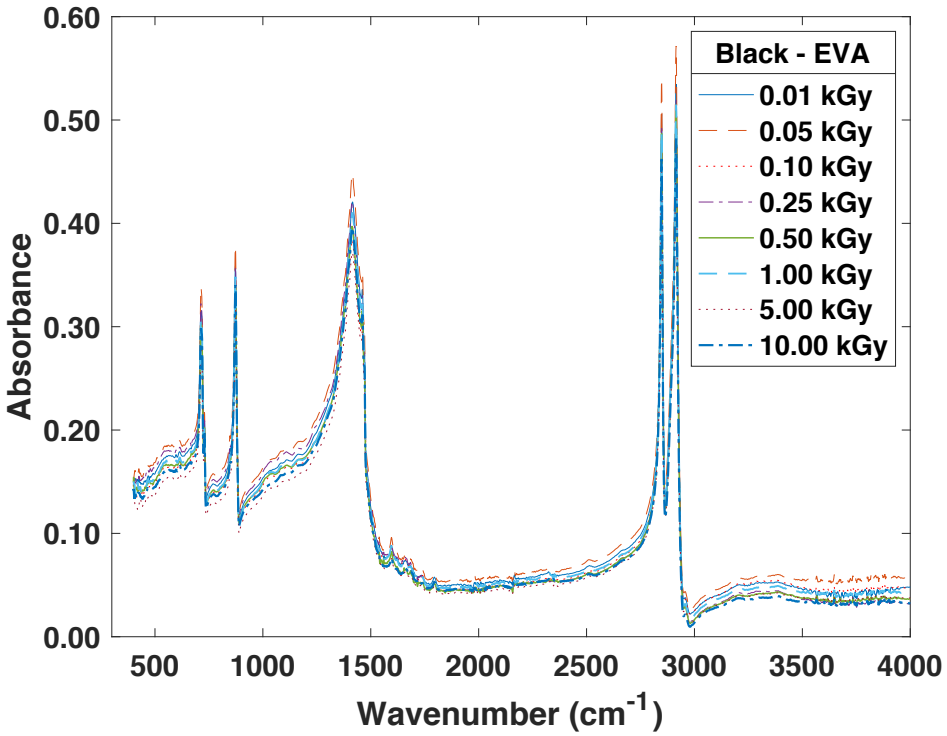

Figure 1: *FTIR spectra, absorbance versus wavenumber, for EVA samples: a) Green, b) White and c) Black, irradiated with absorbed doses from 0.01 kGy to 10.0 kGy (^{60}Co source). The uncertainty obtained was lower than 1%.*

The results for the linearity *versus* wavenumber for EVA samples: a) green, b) white and c) black are shown in Figures 2a, 2b and 2c, respectively. The maximum values for linearity (R^2) were: 0.8839, 0.6422 and 0.5833 for green, white, and black EVA samples, for the wavenumbers 431 cm^{-1}, 2168 cm^{-1} and 1561 cm^{-1}, respectively. From these results it can be inferred that the best EVA sample color is the green one; and the linearity occurs in three different wavenumbers.

a)

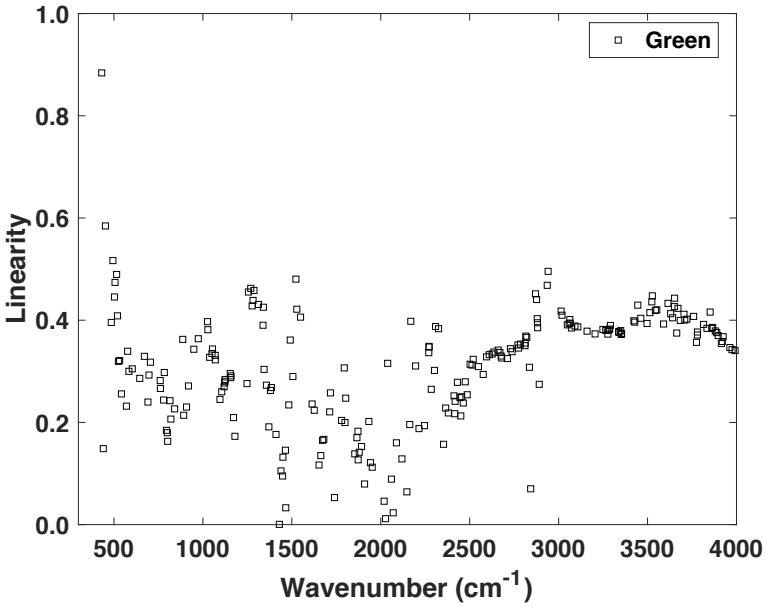

b)

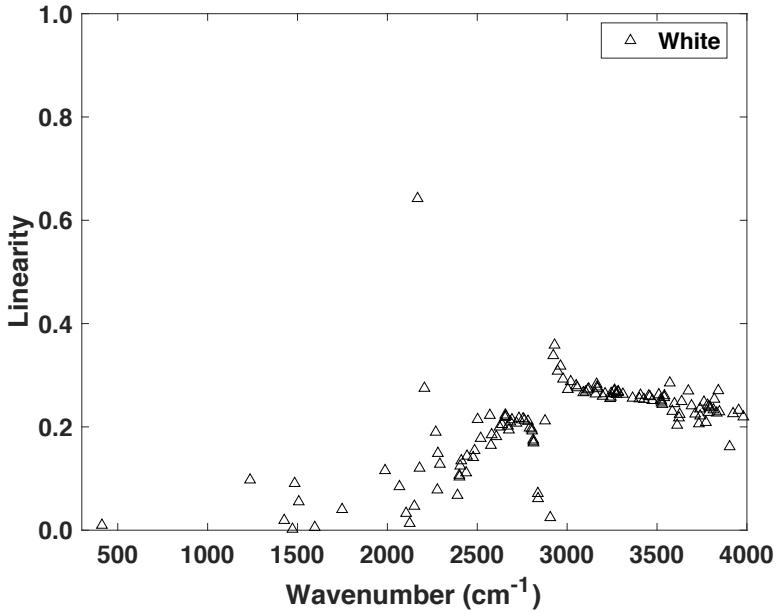

c)

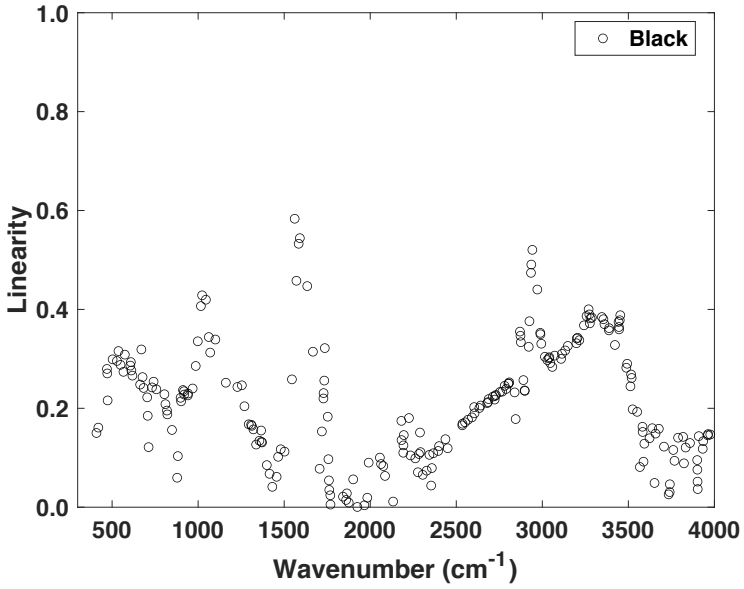

Figure 2: *Linearity versus wavenumber for EVA samples: a) Green, b) White and c) Black. The uncertainty obtained was lower than 1%.*

In Figures 3a, 3b and 3c is presented the normalized sensitivity *versus* wavenumber for EVA samples for all colors. The maximum normalized sensitivities equal to the unit (1) were obtained for the wavenumbers: 418 cm^{-1}, 401 cm^{-1} and 2161 cm^{-1}, for green, white, and black samples, respectively. The region between 400 cm^{-1} and 450 cm^{-1} may be associated with the best values for linearity and normalized sensitivity for the green color; for other regions and sample colors this fact does not occur.

a)

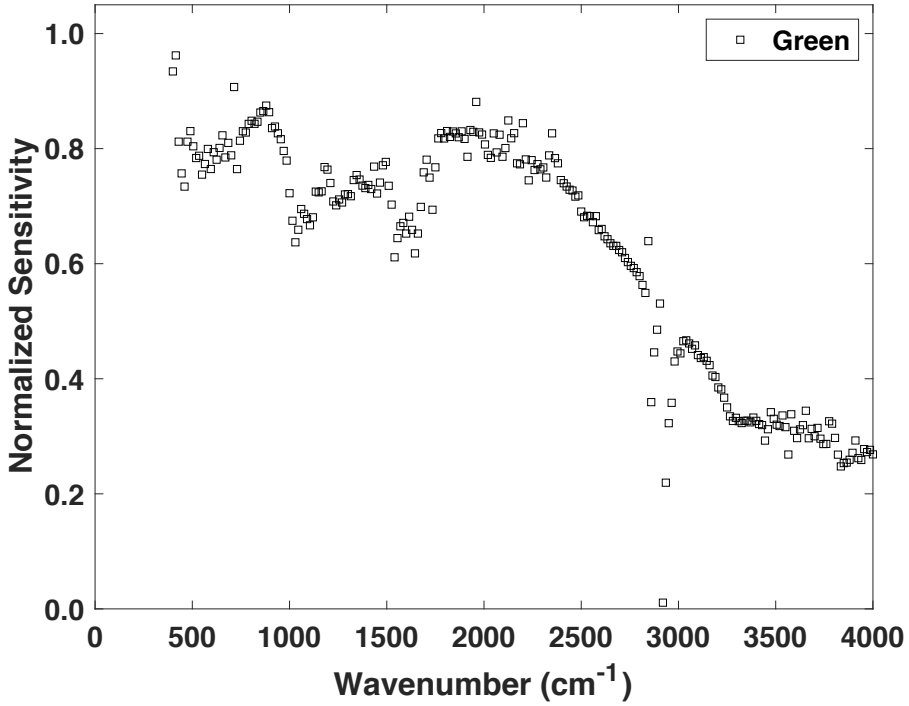
Green
Normalized Sensitivity
Wavenumber (cm-1)
0.0
0.2
0.4
0.6
0.8
1.0
0
500
1000
1500
2000
2500
3000
3500
4000

b)

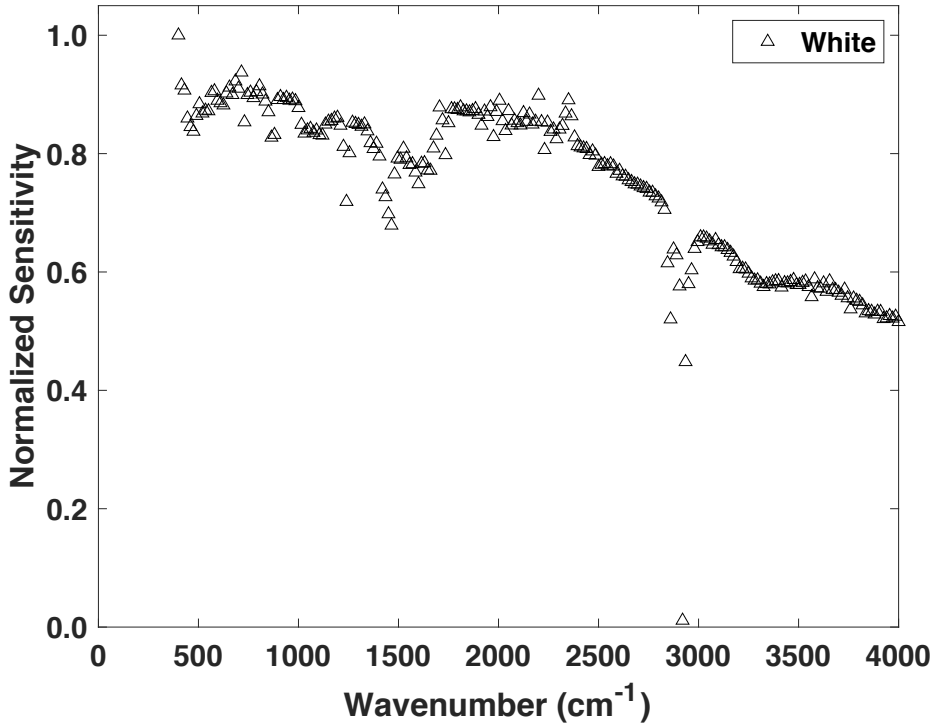
White
Normalized Sensitivity
Wavenumber (cm-1)
0.0
0.2
0.4
0.6
0.8
1.0
0
500
1000
1500
2000
2500
3000
3500
4000

c)

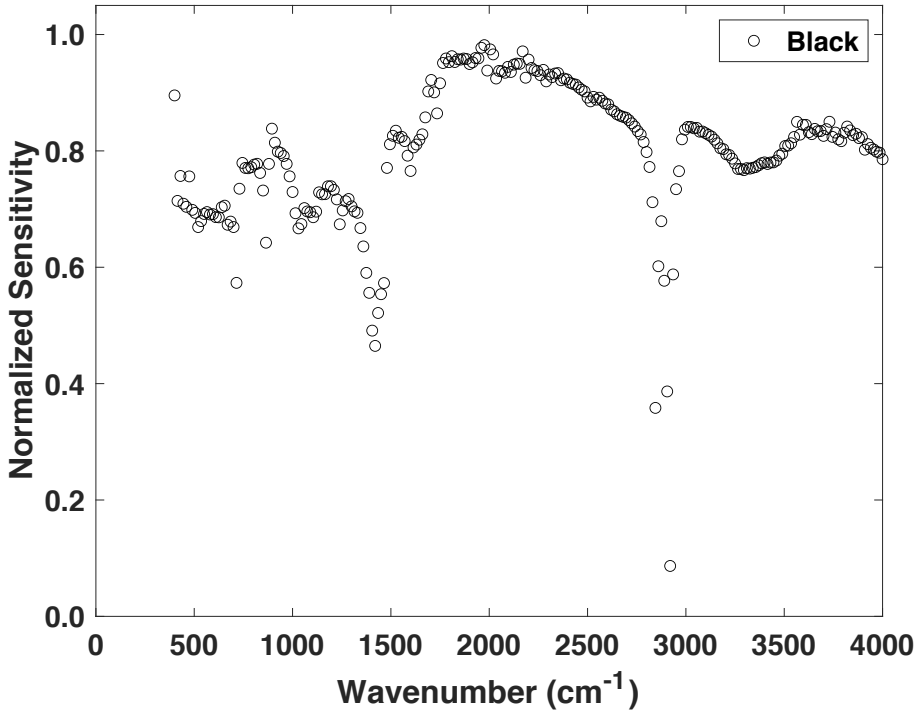

Figure 3: *Normalized sensitivity versus wavenumber for EVA samples: a) Green, b) White and c) Black. The uncertainty obtained was lower than 1%.*

Predicted absorbed dose *versus* absorbed dose data are shown in Figure 4, for the PCR method, for EVA samples of all colors. The R^2 obtained was 1.000 for the PCR method. It can be inferred that these methods are a good alternative, in the applications that require assessing linearity response in dosimetry, since the measurements from each kind of sample may be transformed in linear results. Consequently, these methods can be associated with other characteristics from medical physics as: reproducibility, fading, spatial resolution and others.

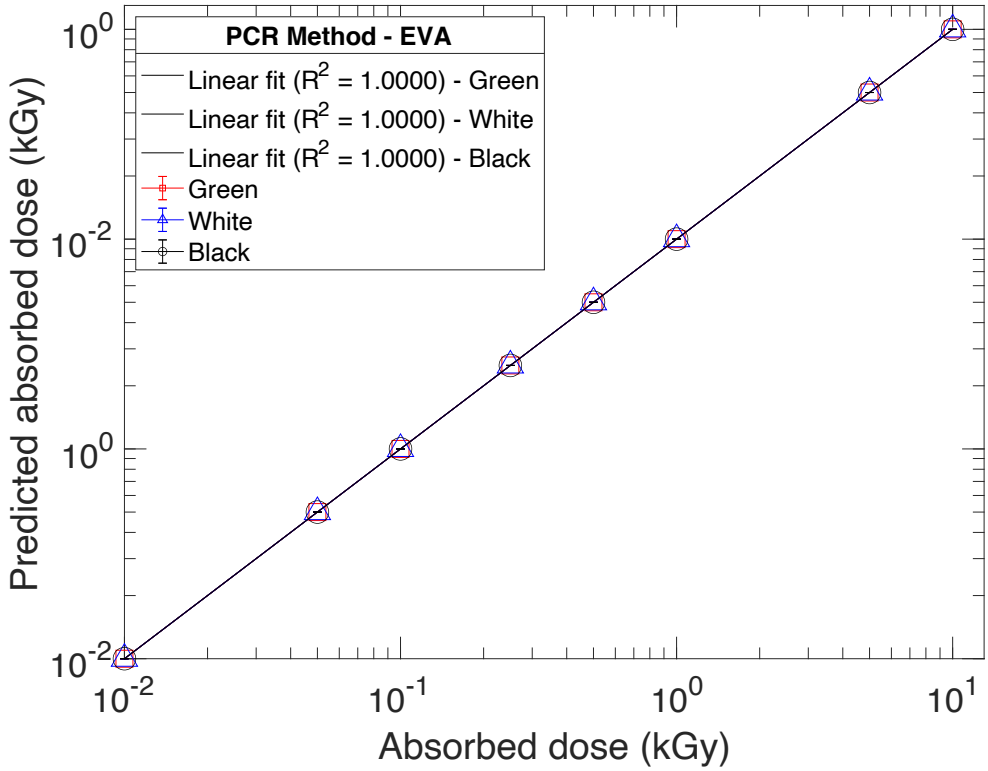

Figure 4: *Application of the PCR method: Predicted absorbed dose versus absorbed dose for: Green, White and Black EVA samples. The uncertainty obtained was lower than 1%.*

Figure 5 shows the Mean-Squared Error (MSE) *versus* the number of principal components (k) with PCR methods for green, white, and black EVA samples. As the number of principal components increased, the MSE decreased for all EVA sample colors applying the PCR method. These results occur because the predicted values are increasingly closer to the actual values. For the value of $k = 8$, all colors of the EVA samples reached zero MSE, thus corresponding to the efficiency of the method. For the $k = 7$ component, the MSE values are: 0.1097, 0.1260 and 0.6265, for the green, white and black colors, respectively. Thus, the sample that shows the lowest values for MSE is the green one.

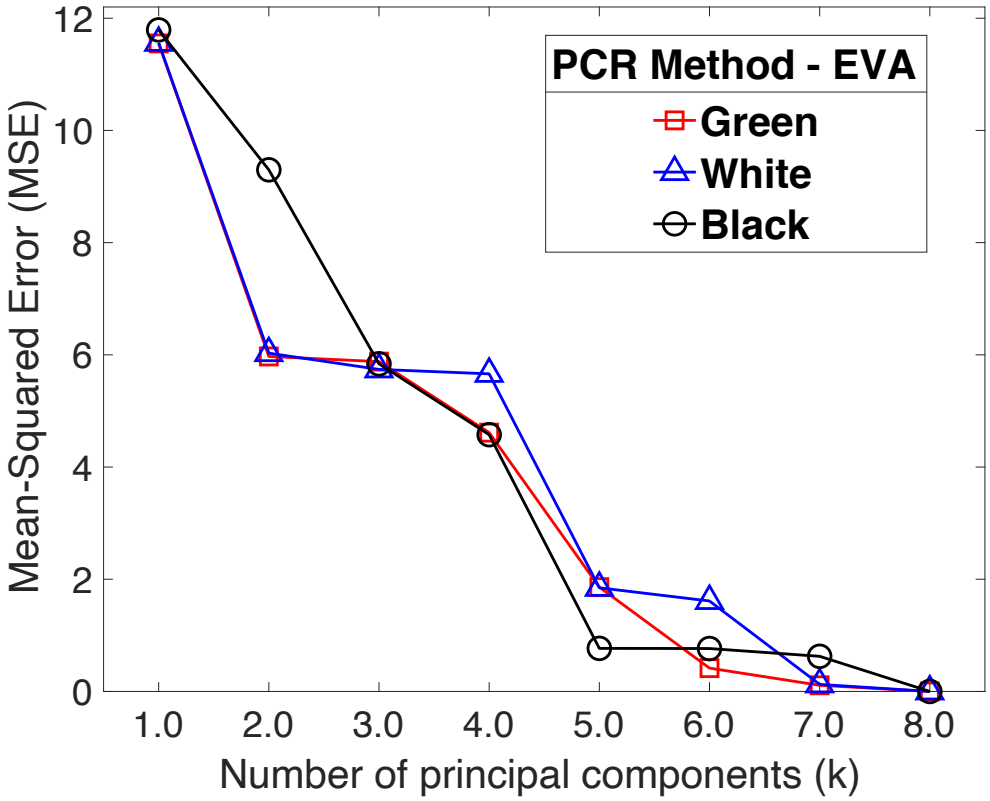

Figure 5: *Mean-Squared Error (MSE) versus number of principal components (k) with PCR methods for green, white and black EVA samples. The uncertainty obtained was lower than 1%.*

In Figure 6 are shown the residuals *versus* absorbed dose for: green, white and black EVA samples respectively, for the number of principal components (k) of $k = 1$, $k = 4$ and $k = 8$, using the PCR method.

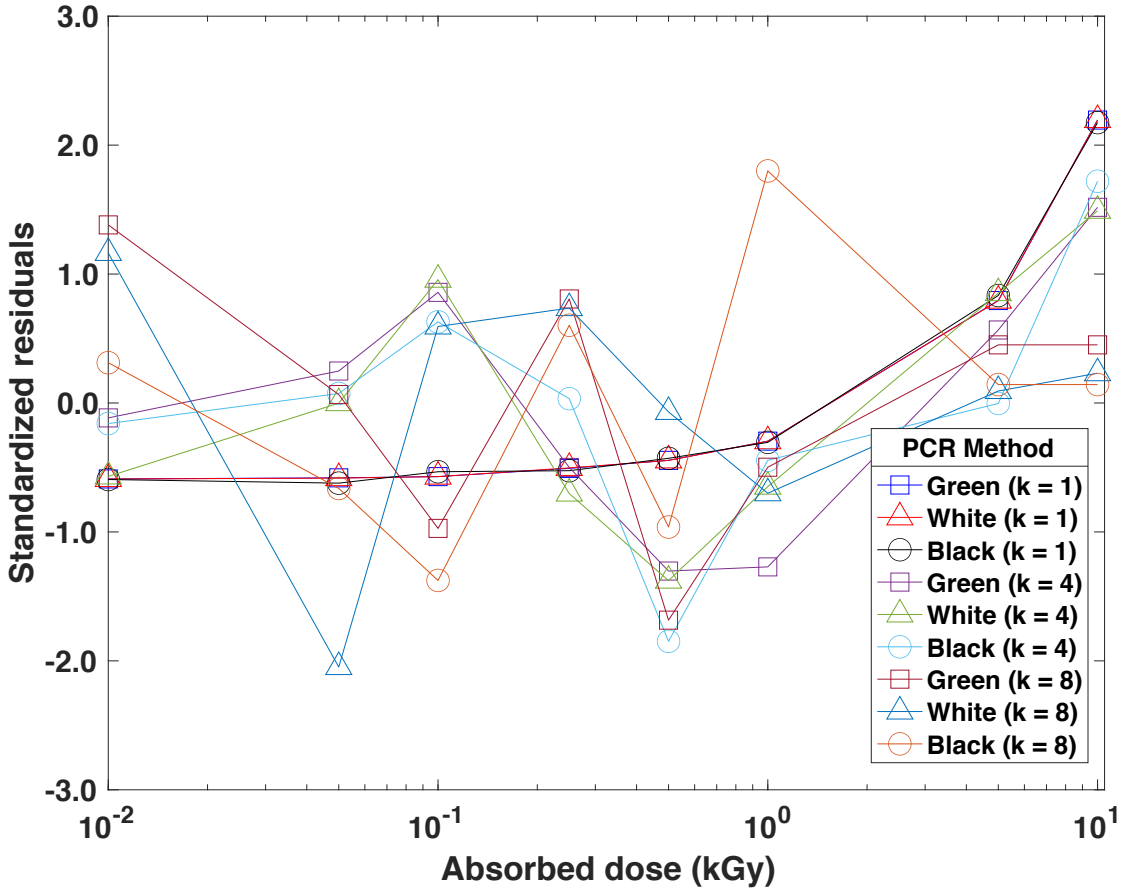

Figure 6: *Residuals versus absorbed dose for EVA samples: Green, White, Black, for the number of principal components (k): k =1, k = 4 and k = 8. The uncertainty obtained was lower than 1%.*

Based on Figure 6, for k = 1, it can be inferred that the residuals for low absorbed doses is < -0.6217, but for the last two doses (5.0 kGy and 10.0 kGy), this residual value is quite high > 2.1944 for all sample colors. In the k = 4 case, there is an alternation between the highest values of residuals associated with colors up to the dose of 0.5 kGy, with the largest residual equal to -1.8484 for the black EVA samples, after the biggest error for the last two doses (5.0 kGy and 10.0 kGy) are 0.8520 and 1.7199, for white and black sample colors, respectively. As the method will use all components k = 8, it has the smallest residual value for all components analyzed as < 0.4508, so the reduction occurs for k = 8, showing the PCR method as the best to be applied in characterizing the linearity of EVA samples of the colors tested in this work.

4. CONCLUSION

After evaluating the EVA samples in three different colors and applying the PCR method, the following conclusions were observed: i) as EVA samples were constituted as solid-state radiation detectors, the FTIR technique proved to be suitable for measurements seeking to characterize the linear response; ii) ranking simultaneously the results through linearity, sensitivity and MSE criteria, the color that predominated with the best results was green, followed by white and black respectively; iii) the PCR method can be applied to assess linearity problems in dosimeters with a view to medical physics. Therefore, EVA samples can be considered as a promising material available for measurements of high doses of gamma radiation.

ACKNOWLEDGMENTS

The authors thank the Brazilian funding agencies CNPq (Projects 104486/2019-8, 164981/2020-9, 151945/2019-5 and 301335/2016-8) and FAPESP (Projects 2018/05982-0 and 2014/12732-9) for partial financial support.

REFERENCES

[1] AHMED, J.; WU, J.; MUSHTAQ, S.; ZHANG, Y. Effects of electron beam irradiation and multi-functional monomer/co-agents on the mechanical and thermal properties of ethylene-vinyl acetate copolymer/polyamide blends. **Mater Today Commun,** v. 23, p. 1-7, 2020.

[2] BARTOLOMEI, S.S.; SANTANA, J.G.; VALENZUELA DÍAZ, F.R.; KAVAKLI, P.A.; GUVEN, O.; MOURA, E.A.B. Investigation of the effect of titanium dioxide and clay grafted with glycidyl methacrylate by gamma radiation on the properties of EVA flexible films. **Radiat Phys Chem**, v. 169, p. 1-9, 2020.

[3] BEE, S.T.; SIN, L.T.; HOE, T.T.; RATNAM, C.T.; BEE, S.L.; RAHMAT, A.R. Study of montmorillonite nanoparticles and electron beam irradiation interaction of ethylene vinyl acetate (EVA)/de-vulcanized waste rubber thermoplastic composites. **Nucl Instrum Meth Phys Res B Beam Interact Mater At,** v. 423, p. 97-110, 2018.

[4] ENTEZAM, M.; AGHJEH, M.K.R.; GHAFFARI, M. Electron beam irradiation induced compatibilization of immiscible polyethylene/ethylene vinyl acetate (PE/EVA) blends: Mechanical properties and morphology stability. **Radiat Phys Chem**, v. 131, p. 22-27, 2017.

[5] RAMARAD, S.; RATNAM, C.T.; KHALID, M.; CHUAH, A.L.; HANSON, S. Improved crystallinity and dynamic mechanical properties of reclaimed waste tire rubber/EVA blends under the influence of electron beam irradiation. **Radiat Phys Chem**, v. 130, p. 362-370, 2017.

[6] VOGT, M.R.; HOLST, H.; SCHULTE-HUXEL, H.; BLANKEMEYER, S.; WITTECK, R.; HINKEN, D.; WINTER, M.; MIN, B.; SCHINKE, C.; AHRENS, I.; KÖNTGES, M.; BOTHE, K.; BRENDEL, R. Optical Constants of UV Transparent EVA and the Impact on the PV Module Output Power under Realistic Irradiation. **Energy Procedia**, v. 92, p. 523-530, 2016.

[7] DINESH, M.; CHIKKAKUNTAPPA, R. Microwave irradiation induced modifications on the interfaces in SAN/EVA/PVC and PVAc/BPA/PVP ternary polymer blends: Positron lifetime study. **Nucl Instrum Meth Phys Res B Beam Interact Mater At,** v. 310, p. 67-74, 2013.

[8] JI, Y.Y.; CHANG, H.S.; LIM, T.; LEE, W. Application of a SrI_2 (Eu) scintillation detector to in situ gamma-ray spectrometry in the environment. **Radiat Meas,** v. 122, p. 67-72, 2019.

[9] KARAKIROVA, Y.; LUND, E.; YORDANOV, N.D. EPR and UV investigation of sucrose irradiated with nitrogen ions and gamma-rays. **Radiat Meas,** v. 43, p. 1337-1342, 2008.

[10] OLIVEIRA, L.N.; NASCIMENTO, E.O.; SCHIMIDT, F.; ANTONIO, P.L.; CALDAS, L.V.E. Characterization of lithium diborate, sodium diborate and commercial soda-lime glass exposed to gamma radiation via linearity analyses. **Radiat Phys Chem,** v. 155, p. 133-137, 2019.

[11] KUMAR, N.; JAIN, P.K.; TANDON, P.; PANDEY, P.M. The effect of process parameters on tensile behavior of 3D printed flexible parts of ethylene vinyl acetate (EVA), **J Manuf Process,** v. 35, p. 317-326, 2018.

[12] OSMAN, A.F.; TUTY, T.F.; RAKIBUDDIN, M.; HASHIM, F.; TUAN JOHARI, S.A.T.; ANANTHAKRISHNAN, R.; RAMLI, R. Pre-dispersed organo-montmorillonite (organo-MMT) nanofiller: Morphology, cytocompatibility and impact on flexibility, toughness and biostability of biomedical ethyl vinyl acetate (EVA) copolymer. **Mater Sci Eng C,** v. 74, p. 194-206, 2017.

[13] GOULAS, A.E.; RIGANAKOS, K.A.; KONTOMINAS, M.G. Effect of ionizing radiation on physicochemical and mechanical properties of commercial multilayer coextruded flexible plastics packaging materials. **Radiat Phys Chem**, v. 68, p. 865–872, 2003.

[14] YAN, K.; TIAN, S.; CHEN, J.; LIU, J. High temperature rheological properties of APAO and EVA compound modified asphalt. **Constr Build Mater,** v. 233, p. 1-11, 2020.

[15] GOUVÊA, R.F.; ANDRADE, C.T. Testing the effect of imidazolium ionic liquid and citrate derivative on the properties of graphene-based PHBV/EVA immiscible blend. **Polym Test,** v. 89, p. 1-9, 2020.

[16] WAHAB, A.; SATTAR, H.; ASHRAF, A.; HUSSAIN, S.N.; SALEEM, M.; MUNIR, S. Thermochemical, kinetic and ash characteristics behaviour of Thar Lignite, agricultural residues and synthetic polymer waste (EVA). **Fuel**, v. 266, p. 1-10, 2020.

[17] SUMAN, S.K.; KADAM, R.M.; MONDAL, R.K.; MURALI, S.; DUBEY, K.A.; BHARDWAJ Y.K.; NATARAJAN, V. Melt-compounded composites of ethylene vinyl acetate with magnesium sulfate as flexible EPR dosimeters: Mechanical properties, manufacturing process feasibility and dosimetric characteristics. **Appl Radiat Isot,** v. 121, p. 1-5, 2017.

[18] BAGHANI, H.R.; ROBATJAZI, M.; MAHDAVI, S.R.; HOSSEINI AGHDAM, S.R. Evaluating the performance characteristics of some ion chamber dosimeters in high dose per pulse intraoperative electron beam radiation therapy. **Phys Med,** v. 58, 81-89, 2019.

[19] HSU, S.M.; YANG, H.W.; YEH, T.C.; HSU, W.L.; WU, C.H.; LU, C.C.; CHEN, W.L.; HUANG, D.Y.C. Synthesis and physical characteristics of radiophotoluminescent glass dosimeters, **Radiat Meas,** v. 42, p. 621-624, 2007.

[20] JENG, C.C.; YUNG, S.W.; LEE, J.H.; SUN, S.S.; YANG, S.H.; HSU, S.M. The readout characteristics of self-fabricated radiophotoluminescent glass dosimeter reading system. **Radiat Meas,** v. 90, p. 210-213, 2016.

[21] SOMMER, M.; FREUDENBERG, R.; HENNIGER, J. New aspects of a BeO-based optically stimulated luminescence dosimeter. **Radiat Meas,** v. 42, p. 617-620, 2007.

[22] ZHYDACHEVSKII, Y.; SUCHOCKI, A.; BERKOWSKI, M.; ZAKHARKO, Y. Optically stimulated luminescence of $YAlO_3:Mn^{2+}$ for radiation dosimetry. **Radiat Meas,** v. 42, p. 625-627, 2007.

[23] ANTONELLO, M.; CACCIA, M.; FERRARI, R.; FRANCHINO, S.; GAUDIO, G.; HAUPTMAN, J.; LEE, S.; PEZZOTTI, L.; SALVATORE, F.; SANTORO, R.; VIVARELLI, I.; WIGMANS, R. Linearity response measurement of a SiPM-based dual-readout calorimeter for future leptonic colliders. **Nucl Instrum Meth A,** v. 958, p. 1-4, 2020.

[24] CARVAJAL, M.A.; VILCHES, M.; GUIRADO, D.; LALLENA, A.M.; BANQUERI, J.; PALMA, A.J. Readout techniques for linearity and resolution improvements in MOSFET dosimeters, **Sens Actuator A Phys,** v. 157, p. 178-184, 2010.

[25] BOS, A.J.J. High sensitivity thermoluminescence dosimetry. **Nucl Instrum Meth Phys Res B Beam Interact Mater At,** v. 184, p. 3-28, 2001.

[26] DESHPANDE, S.; GEURTS, M.; VIAL, P.; METCALFE, P.; HOLLOWAY, L. Sensitivity evaluation of two commercial dosimeters in detecting Helical TomoTherapy treatment delivery errors. **Phys Med**, v. 37, 68-74, 2017.

[27] TAÑO, J.E.; HAYASHI, GONZALES, C.A.B.; YASUDA, H. Effect of the glucono-δ-lactone concentration on the sensitivity and stability of PVA-GTA-I radiochromic gel dosimeter. **Radiat Meas,** v. 134, p. 1-5, 2020.

[28] CHENG, J.; MINGYAO, A.I. Optimal designs for panel data linear regressions, **Stat Probab Lett,** v. 163, p. 1-8, 2020.

[29] HUANG, G.; CHEN, XIAOJING; LI, L.; YUAN, L.; SHI, W. Domain adaptive partial least squares regression. **Chemometr Intell Lab Syst,** v. 201, p. 1-9, 2020.

[30] QIN, L.T.; LIU, S.S.; LIU, H.L.; TONG, J. Comparative multiple quantitative structure-retention relationships modeling of gas chromatographic retention time of essential oils using multiple linear regression, principal component regression, and partial least squares techniques, **J Chromatogr A,** v. 1216, p. 5302-5312, 2009.

[31] SHAKYA, P.R.; MELAKU, Y.A.; PAGE, A.; GILL, T.K. Association between dietary patterns and adult depression symptoms based on principal component analysis, reduced-rank regression and partial least-squares. **Clin Nutr,** v. 39, p. 2811-2823, 2020.

[32] BATISTA BRAGA, J.W.; ALLEGRINI, F.; OLIVIERI, A.C. Maximum likelihood unfolded principal component regression with residual bilinearization (MLU-PCR/RBL) for second-order multivariate calibration. **Chemometr Intell Lab Syst,** v. 170, p. 51-57, 2017.

[33] OLIVEIRA, L.N.; NASCIMENTO, E.O.; MORAIS JÚNIOR, P.A.; ANTONIO, P.L; CALDAS, L.V.E. Evaluation of high-linearity bone radiation detectors exposed to gamma-rays via FTIR measurements. **Appl Radiat Isot**, v. 170, p. 1-6, 2021.

[34] BERTRAND, D.; QANNARI, E.M.; VIGNEAU, E. Latent root regression analysis: an alter native method to PLS. **Chemometr Intell Lab Syst,** v. 58, p. 227-234, 2001.

[35] KÖKSOY, O. Multiresponse robust design: Mean square error (MSE) criterion. **Appl Math Comput,** v. 175, p. 1716-1729, 2006.

[36] MARCILLA, A.; GÓMEZ, A.; MENARGUES, S. TG/FTIR study of the thermal pyrolysis of EVA copolymers. **J Anal Appl Pyrolysis**, v. 74, p. 224-230, 2005.